



## DNA-Containing Exosomes Derived from Cancer Cells Treated with Topotecan Activate a STING-Dependent Pathway and Reinforce Antitumor Immunity

This information is current as of August 4, 2022.

Yuichi Kitai, Takumi Kawasaki, Takuya Sueyoshi, Kouji Kobiyama, Ken J. Ishii, Jian Zou, Shizuo Akira, Tadashi Matsuda and Taro Kawai

*J Immunol* 2017; 198:1649-1659; Prepublished online 9 January 2017;  
doi: 10.4049/jimmunol.1601694  
<http://www.jimmunol.org/content/198/4/1649>

**Supplementary Material** <http://www.jimmunol.org/content/suppl/2017/01/06/jimmunol.1601694.DCSupplemental>

**References** This article **cites 56 articles**, 16 of which you can access for free at:  
<http://www.jimmunol.org/content/198/4/1649.full#ref-list-1>

### Why *The JI*? [Submit online.](#)

- **Rapid Reviews! 30 days\*** from submission to initial decision
- **No Triage!** Every submission reviewed by practicing scientists
- **Fast Publication!** 4 weeks from acceptance to publication

*\*average*

**Subscription** Information about subscribing to *The Journal of Immunology* is online at:  
<http://jimmunol.org/subscription>

**Permissions** Submit copyright permission requests at:  
<http://www.aai.org/About/Publications/JI/copyright.html>

**Email Alerts** Receive free email-alerts when new articles cite this article. Sign up at:  
<http://jimmunol.org/alerts>

# DNA-Containing Exosomes Derived from Cancer Cells Treated with Topotecan Activate a STING-Dependent Pathway and Reinforce Antitumor Immunity

Yuichi Kitai,<sup>\*,†</sup> Takumi Kawasaki,<sup>†</sup> Takuya Sueyoshi,<sup>†</sup> Kouji Kobiyama,<sup>‡,§,1</sup>  
Ken J. Ishii,<sup>‡,§</sup> Jian Zou,<sup>¶,||</sup> Shizuo Akira,<sup>¶,||</sup> Tadashi Matsuda,<sup>\*</sup> and Taro Kawai<sup>†</sup>

**Danger-associated molecular patterns derived from damaged or dying cells elicit inflammation and potentiate antitumor immune responses. In this article, we show that treatment of breast cancer cells with the antitumor agent topotecan (TPT), an inhibitor of topoisomerase I, induces danger-associated molecular pattern secretion that triggers dendritic cell (DC) activation and cytokine production. TPT administration inhibits tumor growth in tumor-bearing mice, which is accompanied by infiltration of activated DCs and CD8<sup>+</sup> T cells. These effects are abrogated in mice lacking STING, an essential molecule in cytosolic DNA-mediated innate immune responses. Furthermore, TPT-treated cancer cells release exosomes that contain DNA that activate DCs via STING signaling. These findings suggest that a STING-dependent pathway drives antitumor immunity by responding to tumor cell-derived DNA. *The Journal of Immunology*, 2017, 198: 1649–1659.**

Innate immunity is the first line of host defense against pathogen infection and involves the recognition of conserved molecular structures called pathogen-associated molecular patterns (PAMPs) by pattern-recognition receptors (PRRs), such as

TLRs, RIG-I-like receptors (RLRs), DNA sensors, Nod-like receptors, and C-type lectin receptors (1). Signaling through PRRs results in the induction of inflammatory responses that are required for the initial elimination of pathogens and activation of pathogen-specific adaptive immunity. In addition to their function as PAMP receptors, recent studies revealed that PRRs respond to endogenous alarmin or danger-associated molecular patterns (DAMPs) that are released by dying, damaged, or infected cells; these include extracellular ATP, extracellular matrix, heat shock proteins, S100 proteins, nucleic acids (genomic DNA, mitochondrial DNA, small RNA, mRNA, RNPs), nuclear chromatin-binding proteins (HMGB1, histones), mitochondrial reactive oxygen species, and uric acid (2–6). These DAMPs trigger inflammation and tissue repair but are also involved in chronic inflammatory diseases and autoimmunity.

DAMPs play important roles in shaping adaptive immune responses through the activation of innate immune cells, such as dendritic cells (DCs) and macrophages. It was shown that HMGB1 released from viral RNA-stimulated cells promotes the activation of DCs and contributes to enhanced Th1 responses (7). Moreover, DAMPs trigger antitumor immunity. HMGB1 and HSP90 are secreted by dying cancer cells after treatment with the anti-cancer drug doxorubicin and activate TLR4–MyD88 signaling pathways (8, 9). Simultaneously, dying cell-derived ATP activates the NLRP3 inflammasome (5). These responses induce the expression and maturation of IL-1 $\beta$ , which mediates recruitment of various immune cells to the tumors and shapes the immune response to tumors. Moreover, it was shown that radiation triggers the death of tumor cells and the production of oxidized DNA, which activates DCs via the STING-dependent signaling pathway (10). STING is an essential signaling molecule for the production of cytokines and type I IFNs in response to pathogen-derived DNA and is activated by its ligand, cyclic GMP-AMP (cGAMP). cGAMP is synthesized from GTP and ATP by cyclic GMP-AMP synthase (cGAS) following its association with pathogenic DNA, and the cGAS–STING axis activates the transcription factors NF- $\kappa$ B and IRF3 to induce the expression of inflammatory cytokines and type I IFNs, respectively (11). STING-deficient mice exhibit augmented tumor growth due to the attenuation of antitumor T cell

<sup>\*</sup>Department of Immunology, Graduate School of Pharmaceutical Sciences, Hokkaido University, Sapporo, Hokkaido 060-0812, Japan; <sup>†</sup>Laboratory of Molecular Immunobiology, Graduate School of Biological Sciences, Nara Institute of Science and Technology, Ikoma, Nara 630-0192, Japan; <sup>‡</sup>Laboratory of Vaccine Science, Immunology Frontier Research Center, Osaka University, Suita, Osaka 565-0871, Japan; <sup>§</sup>Laboratory of Adjuvant Innovation, National Institutes of Biomedical Innovation, Health and Nutrition, Ibaraki, Osaka 567-0085, Japan; <sup>¶</sup>Laboratory of Host Defense, Immunology Frontier Research Center, Osaka University, Suita, Osaka 565-0871, Japan; and <sup>||</sup>Department of Host Defense, Research Institute for Microbial Diseases, Osaka University, Suita, Osaka 565-0871, Japan

<sup>1</sup>Current address: Division of Inflammation Biology, La Jolla Institute for Allergy and Immunology, La Jolla, CA.

ORCID: 0000-0002-6728-3872 (K.J.I.).

Received for publication October 3, 2016. Accepted for publication December 5, 2016.

This work was supported by Ministry of Education, Culture, Sports, Science and Technology KAKENHI Grants-in-Aid for Scientific Research on Innovative Areas (15H01381; to T. Kawai) and Research Activity Start-Up (15H05994; to Y.K.), as well as by the Uehara Memorial Foundation (to T. Kawai) and the Mochida Memorial Foundation for Medical and Pharmaceutical Research (to T. Kawai).

Y.K., J.Z., and T.S. performed experiments; Y.K., T. Kawasaki, and T. Kawai designed experiments; K.K., K.J.I., S.A., and T.M. analyzed data; Y.K. and T. Kawai wrote the manuscript; and T. Kawai supervised the project. All authors analyzed the results and approved the final version of the manuscript.

The microarray data presented in this article have been submitted to the Gene Expression Omnibus (<https://www.ncbi.nlm.nih.gov/geo/query/acc.cgi?acc=GSE90042>) under accession number GSE90042.

Address correspondence and reprint requests to Prof. Taro Kawai, Laboratory of Molecular Immunobiology, Graduate School of Biological Sciences, Nara Institute of Science and Technology, 8916-5 Takayama-cho, Ikoma, Nara 630-0192, Japan. E-mail address: tarokawai@bs.naist.jp

The online version of this article contains supplemental material.

Abbreviations used in this article: cGAMP, cyclic GMP-AMP; cGAS, cyclic GMP-AMP synthase; CM, conditioned medium; DAMP, danger-associated molecular pattern; DC, dendritic cell; DKO, double-KO; GM-DC, GM-CSF-induced DC; ISD, IFN stimulatory DNA; KO, knockout; MEF, mouse embryonic fibroblast; PAMP, pathogen-associated molecular pattern; PI, propidium iodide; polyI:C, polyinosinic-polycytidylic acid; PRR, pattern-recognition receptor; qPCR, quantitative PCR; RLR, RIG-I-like receptor; RT, room temperature; shRNA, short hairpin RNA; TPT, topotecan; WT, wild-type.

Copyright © 2017 by The American Association of Immunologists, Inc. 0022-1767/17/\$30.00

activation during radiation treatment (12, 13). Moreover, intratumoral administration of cGAMP inhibits tumor growth in a murine melanoma model (14). Therefore, DAMPs are therapeutically important molecules that act as adjuvants to induce effective immune responses to infectious agents and tumors.

In this study, we screened various antitumor agents for their ability to modulate antitumor immune responses and found that toptecan (TPT) could trigger the secretion of DAMPs, which are responsible for activation of DCs, from cancer cell lines. TPT is a camptothecin analog that inhibits topoisomerase I and induces cell death of proliferating tumor cells by triggering DNA double-strand breaks and DNA damage responses; it is used as a second line of chemotherapy against ovarian and small cell lung cancer (15). TPT inhibited tumor growth by promoting DC maturation and CD8<sup>+</sup> T cell activation in tumor-bearing mice. Notably, the antitumor effects of TPT decreased in *Sting<sup>gt/gt</sup>* mice, which have a loss-of-function mutation at the ligand-binding site of STING (16). TPT treatment triggered the secretion of exosomes containing immunostimulatory DNA, which were taken up by DCs and activated a STING-dependent pathway. Thus, these findings suggest that cancer cell DNA released by TPT treatment has the potential to act as an adjuvant that elicits STING-dependent antitumor immunity.

## Materials and Methods

### Animals

All animals were kept under specific pathogen-free conditions. Wild-type (WT) C57BL/6 mice were purchased from CLEA Japan (Osaka, Japan). MyD88-knockout (KO), TRIF-KO, TLR2-KO, TLR4-KO, and IPS-1-KO mice were prepared as described previously (17–21). IRF3-KO mice were purchased from the RIKEN BioResource Center (22). *Sting<sup>gt/gt</sup>* mice were purchased from the Jackson Laboratory (Bar Harbor, ME) (16). These mice were backcrossed onto a C57BL/6 background for more than eight generations. All animal experiments were performed with the approval of the Animal Research Committee of Nara Institute of Science and Technology.

### Reagents and cells

LPS and polyinosinic-polycytidylic acid (polyI:C) were purchased from InvivoGen. Antitumor drugs and murine rIFN- $\beta$  were purchased from Sigma. Nec-1 was purchased from Cayman Chemical. GSK'872 was purchased from Calbiochem. Z-VAD was purchased from MBL. Nigericin was purchased from WAKO. Sense and anti-sense IFN stimulatory DNA (ISD) sequences were synthesized (Grainer Japan) and annealed (sense; 5'-TACAGATCTACTAGTGATCTATGACTGATCTGTACATGATCTACA-3'). polyI:C and ISD were mixed with Lipofectamine 2000 (Thermo Fisher Scientific) at a 2:1 ratio ( $\mu\text{g}:\mu\text{l}$ ) in Opti-MEM (Thermo Fisher Scientific) for stimulation. E0771 cells were purchased from CH3 BioSystems and cultured in DMEM (Nacalai Tesque) supplemented with 10% FBS (Life Technologies) and 0.05 mM 2-ME (Nacalai Tesque) at 37°C in a humidified 5% CO<sub>2</sub>/95% air atmosphere. GM-CSF-induced DCs (GM-DCs) were prepared by culturing bone marrow cells from femurs and tibias of C57BL/6J mice (female, 8 wk) in RPMI 1640 (Nacalai Tesque) containing 10% FBS, 10 ng/ml GM-CSF, 0.05 mM 2-ME, and penicillin/streptomycin (Nacalai Tesque) for 7 d.

### ELISA

E0771 cells ( $2.0 \times 10^5$  cells per well) were seeded on 96-well plates and treated with antitumor drugs at the indicated concentrations for 72 h at 37°C. After centrifugation,  $2.0 \times 10^5/50 \mu\text{l}$  GM-DCs or  $2.0 \times 10^4/50 \mu\text{l}$  mouse embryonic fibroblasts (MEFs) were cultured with 200  $\mu\text{l}$  of the supernatant (conditioned medium; CM) for 48 h, and IL-6 and CXCL10 production was measured by ELISA, according to the manufacturer's instructions (R&D Systems).

### Apoptosis assay

E0771 cells ( $1.0 \times 10^6$  cells per well) were seeded on six-well plates and treated with 5  $\mu\text{g}/\text{ml}$  TPT for 72 h, and the cells were washed with 10 mM HEPES (pH 7.4), 140 mM NaCl, and 2.5 mM CaCl<sub>2</sub> and stained with APC Annexin V (BD Biosciences) and 1  $\mu\text{g}/\text{ml}$  propidium iodide (PI) (Sigma). Stained cells were analyzed with a BD Accuri (BD Biosciences).

### MTT assay

E0771 cells ( $3.0 \times 10^3$  cells per well) were seeded on 96-well plates and treated with TPT at the indicated concentrations for 72 h, after which cell viability was measured using an MTT Cell Proliferation and Cytotoxicity Assay Kit (BosterBio), according to the manufacturer's instructions.

### Immunoblotting

GM-DCs ( $5.0 \times 10^5$  cells per 125  $\mu\text{l}$ ) were cultured with 500  $\mu\text{l}$  of CM from E0771 cells treated with 5  $\mu\text{g}/\text{ml}$  TPT for the indicated times. The cells were lysed in 50 mM Tris-HCl (pH 8), 150 mM NaCl, 1% Nonidet P-40, 0.5% sodium deoxycholate, and 0.1% SDS. The samples were separated by SDS-PAGE and immunoblotted with anti-IRF3 (D83B9), anti-phospho-IRF3 (Ser<sup>396</sup>, 4D4G), anti-NF- $\kappa$ B p65 (D14E12), anti-phospho-NF- $\kappa$ B p65 (Ser536, 93H1), anti-p38 MAPK, anti-phospho-p38 MAPK (Thr<sup>180</sup>/Tyr<sup>182</sup>), anti-ERK1/2, anti-phospho-ERK1/2 (Thr<sup>202</sup>/Tyr<sup>204</sup>), anti-JNK, anti-phospho-JNK (Thr<sup>183</sup>/Tyr<sup>185</sup>; all from Cell Signaling Technology), anti-STAT1 (E-23; Santa Cruz Biotechnology), anti-phospho-STAT1 (Ser<sup>727</sup>; Cell Signaling Technology), or anti-caspase-1 Ab (M-20; Santa Cruz Biotechnology).

### Quantitative PCR

GM-DCs ( $2.0 \times 10^6$  cells per 500  $\mu\text{l}$ ) were cultured with 2 ml of CM from E0771 cells treated with 5  $\mu\text{g}/\text{ml}$  TPT for 48 h, and total RNA was isolated using TRIzol Reagent (Invitrogen), according to the manufacturer's instructions. cDNA was synthesized from the isolated RNA using ReverTra Ace (TOYOBO) with random hexamer primers, according to the manufacturer's instructions. Semiquantitative analysis of mRNA levels was performed with a LightCycler 96 System (Roche). Primer sets for quantitative PCR (qPCR) analysis are listed in Supplemental Table I.

### Microarray

Total RNA was isolated as for qPCR, and sample cDNA was synthesized and biotinylated using the Ovation RNA Amplification System V2 and Encore Biotin Module (both from NuGEN), according to the manufacturer's instructions. The sample cDNA was hybridized with a GeneChip Mouse Gene 2.0 ST Array (Affymetrix) using an Affymetrix Fluidics Station 450, and the arrays were scanned with a GeneChip Scanner GCS2500 (Hewlett-Packard). Gene expression profiles were analyzed with MAS5.0 (Microarray Suite version 5.0; Affymetrix). Microarray data presented in this article have been submitted to GEO under accession number GSE90042 (<https://www.ncbi.nlm.nih.gov/geo/query/acc.cgi?acc=GSE90042>).

### In vivo tumor progression

E0771 cells ( $3.0 \times 10^6$  cells) were injected into the right flank of C57BL/6 mice (female, 8 wk old). After the tumor volume reached 100 mm<sup>3</sup>, mice were treated with 20 mg/kg TPT (i.p.) every 3 d, and the tumor diameter was measured with a caliper. Tumor volume was calculated using the following formula: volume =  $0.52 \times (\text{width})^2 \times \text{length}$ .

### FACS of tumor-infiltrating cells

An E0771 tumor was established as above, and 40  $\mu\text{l}$  of 1 mg/ml TPT was injected into the tumor after it reached 500 mm<sup>3</sup>. The tumor was dissected 4 d after TPT treatment and dispersed in 3 ml of RPMI 1640 containing 5% FBS, 2 mg/ml Dispase II (Sigma), 0.4 Wünsch unit/ml Liberase TL (Roche), and 1 U/ml DNase I (Promega) for 45 min at 37°C with shaking; subsequently, the cells were treated with 5 mM EDTA for 5 min. After tissue debris was eliminated with a 100- $\mu\text{m}$  cell strainer, the cells were suspended in PBS containing 1% BSA (Sigma) and 2 mM EDTA and incubated with Mouse Fc Block (BD Biosciences) for 30 min on ice. Next, the cells were stained with the following Abs for 30 min on ice: anti-CD45 (HI30; BD Biosciences), anti-Ly-6G (1A8; BD Biosciences), anti-F4/80 (BM8; BioLegend), anti-CD3 (17A2; Tonbo Biosciences), anti-CD4 (GK1.5; Tonbo Biosciences), anti-CD8b (H35-17.2; BD Biosciences), anti-NK1.1 (PK136; BioLegend), anti-CD11c (N418; BioLegend), anti-I-A/I-E (2G9; BD), and anti-CD69 (FN50; BioLegend). After washing twice, the cells were stained with 250 ng/ml 7-amino-actinomycin D for 10 min and then analyzed and sorted with a BD FACSARIA II.

### In vitro DC activation

GM-DCs ( $2.0 \times 10^6$  cells per 500  $\mu\text{l}$ ) were cultured with 2 ml of CM from E0771 cells treated with 5  $\mu\text{g}/\text{ml}$  TPT for 48 h, blocked as above, and stained with anti-I-A/I-E Ab and anti-CD86 Ab (GL-1; BD Biosciences). Stained cells were analyzed with a BD FACSARIA II.

### T cell staining in tumor sections

After TPT injection into an E0771 tumor, the harvested tumor was embedded in OCT compound and frozen with liquid nitrogen; 6- $\mu$ m sections were prepared with a cryostat (CM3050S; Leica). The sections were fixed with 3% paraformaldehyde/PBS for 15 min at room temperature (RT) and then blocked with PBS containing 5% goat serum, 5% FBS, and 0.1% Nonidet P-40 for 30 min at RT. The samples were stained with anti-CD3 $\zeta$  Ab ( $\times 200$  dilution, FL163; Santa Cruz) for 1 h at RT and then stained with anti-rabbit IgG–Alexa Fluor 568 ( $\times 500$  dilution, A11004; Thermo Fisher Scientific) and 0.5  $\mu$ g/ml Hoechst 33342 (Sigma) for 30 min at RT. Stained samples were observed with a confocal microscope (FV10i; Olympus).

### Knockdown

Knockdown of cGAS was performed using short hairpin RNA (shRNA)-expressing retroviral vectors, as described previously (23). shRNA sequences were indicated as described below; scramble shRNA, 5'-GTAAGGCTATGAAGAGATACTTCAAGAGAGTATCTCTTCATAGCCTTAC-3'; cGAS shRNA#1, 5'-GGATTGAGCTACAAGAATATTCAAGAGATATCTTG-TAGCTCAATCC-3'; and cGAS shRNA#2, 5'-GCTGTAAACACTTC-TTATCATTCAAGAGATGATAAGAAGTGTACAGC-3'.

### Exosome purification

To remove exosomes from FBS, FBS was ultracentrifuged for 70 min at 100,000  $\times g$  using an SW 41 Ti Rotor (Beckman Coulter). E0771 cells were grown in DMEM containing 10% exosome-depleted FBS, and  $9.0 \times 10^7$  E0771 cells were seeded on three 150-mm dishes and treated with 5  $\mu$ g/ml TPT for 72 h at 37°C. To remove the cells and their debris, the CM was centrifuged at 500  $\times g$  for 10 min, and the supernatant was further centrifuged at 12,000  $\times g$  for 20 min. The resulting supernatant was filtered through a 0.22- $\mu$ m filter, and the exosomes were recovered by ultracentrifugation at 100,000  $\times g$  for 70 min using an SW 41 Ti Rotor. After washing the pellet with PBS, the sample was further ultracentrifuged as above. The resulting pellet was suspended in PBS, and 40  $\mu$ g of the exosomal protein was separated by SDS-PAGE. CD63, Alix, and GM130 were detected in the sample by immunoblotting using anti-CD63 ( $\times 500$  dilution, H-193; Santa Cruz Biotechnology), anti-Alix ( $\times 1000$  dilution, 3A9; Cell Signaling Technology), and anti-GM130 Ab ( $\times 1000$  dilution, 35/GM130; BD Biosciences).

### DNA purification from CM

CM from TPT-treated E0771 cells was prepared as above, and protein in the CM was removed by phenol/chloroform extraction. The sample was treated with 5  $\mu$ g/ml RNase A for 1 h at 37°C, and the DNA was purified by phenol/chloroform extraction. Purified DNA was stained with SYBR Gold (Thermo Fisher Scientific) following agarose gel electrophoresis and visualized with a UV transilluminator (MID-170; AS ONE).

### Immunofluorescence

Stable STING-expressing MEFs were prepared using pMRX–STING–EGFP–ires–bsr and Plat-E cells, as described previously (24). STING-expressing MEFs were cultured on a cover slip and stimulated with 1  $\mu$ g/ml ISD for 2 h or with CM from TPT-treated E0771 cells for 4 h. The cells were fixed with 3% paraformaldehyde and stained with anti-GM130 Ab ( $\times 300$  dilution, 35/GM130; BD). After washing with PBS, the cells were stained with anti-mouse IgG–Alexa Fluor 568 ( $\times 2000$  dilution) and 0.5  $\mu$ g/ml Hoechst 33342 and observed as above. Plat-E cells and pMRX–ires–bsr were kind gifts from Dr. T. Kitamura (Tokyo University) and Dr. S. Yamaoka (Tokyo Medical and Dental University).

## Results

### TPT-treated E0771 cells release DAMPs that induce IL-6 production by DCs

We developed a screening system to examine whether antitumor drugs have an impact on DC activation via release of DAMPs. We treated the murine breast cancer cell line E0771 with a variety of antitumor drugs (Fig. 1B), transferred the culture supernatants (CM) to murine bone marrow–derived GM-DCs, and measured levels of the inflammatory cytokine IL-6 by ELISA (Fig. 1A). IL-6 production was markedly induced in the supernatant of GM-DCs cultured with CM that had been treated with TPT, an inhibitor of topoisomerase I (Fig. 1B). As reported previously, CM from cells

treated with DMXAA and vinblastine was also capable of inducing IL-6 production, although the levels were lower compared with CM from cells treated with TPT (25, 26). Next, we examined whether TPT directly induces IL-6 production by E0771 cells or GM-DCs. IL-6 was secreted by GM-DCs in the presence of CM from E0771 cells treated with TPT but not when GM-DCs or E0771 cells were exposed to TPT (Fig. 1C), suggesting that CM from TPT-treated E0771 cells contains agonists that cause DCs to produce IL-6. IL-6 was also found in the supernatant of GM-DCs cultured with CM of six other TPT-treated cancer cell lines: HeLa (human cervix adenocarcinoma), A549 (human lung epithelial cells), MCF7 (human breast adenocarcinoma), B16-F10 (murine skin melanoma), LLC (murine Lewis lung carcinoma), and EL4 (murine lymphoma) (Fig. 1D). Furthermore, innate immune cells, including Flt3 ligand–induced DCs, peritoneal macrophages, and M-CSF–induced macrophages, also produced IL-6 in the presence of CM from TPT-treated E0771 cells (Fig. 1E). In addition to IL-6, GM-DCs cultured with CM from TPT-treated E0771 cells produced IFN- $\beta$  and CXCL10 but not IL-1 $\beta$ , IL-18, TNF- $\alpha$ , or IL-33 (Fig. 1F).

Because TPT is known to induce cell death in various cancer cells, we evaluated cell death after TPT treatment by staining cells with annexin V and PI. TPT treatment increased the populations of Annexin V<sup>+</sup> PI<sup>−</sup> and Annexin V<sup>+</sup> PI<sup>+</sup> E0771 cells (Fig. 1G). Furthermore, TPT treatment resulted in growth arrest of E0771 cells, as determined by MTT assay (Fig. 1H). In contrast, TPT did not affect the viability of DCs (data not shown), suggesting that it promotes cell death of proliferating tumor cells.

### DC activation by TPT-treated E0771 cells

Next, we performed a microarray analysis to compare the gene expression profile in GM-DCs cultured with CM from untreated and TPT-treated E0771 cells (Fig. 2A). Genes encoding cytokines (*Il6* and *Ifnb1*), chemokines (*Cxcl9*), and T cell–costimulatory molecules (*Tnfsf10* and *Tnfsf9*) were upregulated in GM-DCs cultured with TPT-treated CM relative to control CM (Fig. 2B). Expression of mRNA for chemokines (*Cxcl9*, *Cxcl11*, and *Cxcl10*) and T cell–costimulatory molecules (*4-1bb1*, *Light*, *Cd301*, *Cd80*, and *Cd86*) was also upregulated, but the expression of T cell–inhibitory molecules (*B7-h1* and *B7-dc*) was not (Fig. 2C, 2D). In addition, surface expression of the activation markers CD86 and I-A/I-E was upregulated on GM-DCs cultured with CM from TPT-treated E0771 cells (Fig. 2E).

We next examined the activation of signaling molecules in response to CM. Stimulation of GM-DCs for 2 h with CM from TPT-treated E0771 cells resulted in phosphorylation of p65 (a component of NF- $\kappa$ B), IRF3, and STAT1 (Fig. 2F, 2G, Supplemental Fig. 1A). Phosphorylation of the MAPKs ERK1/2, p38, and JNK also increased within 15 min after stimulation (Fig. 2H). Although ERK1/2 phosphorylation was comparable in CM- and LPS-stimulated conditions, p38 and JNK phosphorylation was weaker in CM-stimulated cells than in LPS-stimulated cells (Fig. 2H). Taken together, these findings suggest that DC activation is induced by CM from TPT-treated E0771 cells through the activation of NF- $\kappa$ B, IRF3, and MAPKs.

### TPT triggers antitumor immune responses

We evaluated whether TPT enhances antitumor immune responses in vivo. To this end, we injected E0771 cells into C57BL/6 mice to develop tumors before administration of TPT. The tumor volume of TPT-treated mice was lower than that of untreated mice (Fig. 3A, 3B). We then analyzed populations of immune cells infiltrated into tumors by FACS, and found that the ratios of CD3<sup>+</sup> T cells, CD8<sup>+</sup> T cells, neutrophils (Ly-6G<sup>+</sup> F4/80<sup>−</sup>), and DCs (I-A/I-E<sup>+</sup> CD11c<sup>+</sup>)

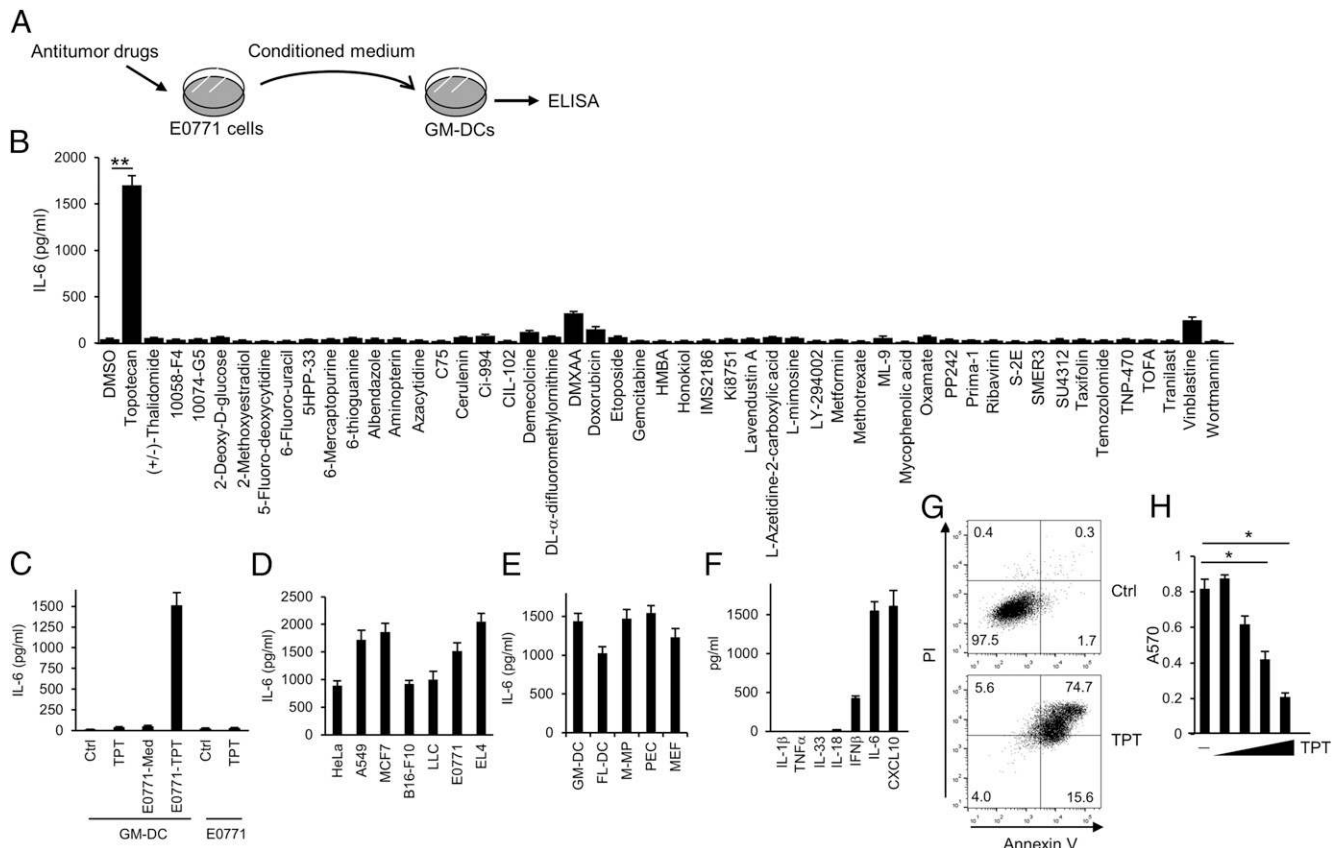


**FIGURE 1.** TPT induces DAMP secretion from tumor cells. **(A)** Schematic representation of the screening for antitumor drugs that induce DAMP secretion. **(B)** E0771 cells were treated with 10  $\mu$ M antitumor drugs for 3 d, after which GM-DCs were cultured with CM from E0771 cells for 48 h. IL-6 production by GM-DCs was determined by ELISA. **(C)** GM-DCs and E0771 cells were cultured with 5  $\mu$ g/ml TPT or CM from TPT-treated E0771 cells for 48 h, and IL-6 production by cells was measured by ELISA. **(D)** Tumor cell lines were treated with 5  $\mu$ g/ml TPT for 3 d, and IL-6 production from GM-DCs was measured as in (C). **(E)** Cells were cultured with CM from TPT-treated E0771 cells for 48 h, and their IL-6 production was determined by ELISA. **(F)** GM-DCs were cultured as in (C), and their cytokine production was determined by ELISA. **(G)** E0771 cells were treated with 5  $\mu$ g/ml TPT for 72 h and then stained with annexin V and PI. Stained cells were analyzed by FACS. **(H)** E0771 cells were treated with 0.01, 0.1, 1, or 10  $\mu$ M TPT for 72 h and then cultured with MTT reagents for 2 h. The absorbance at 570 nm was measured.  $n = 3$ ; mean values and SEs are depicted. \* $p < 0.05$ , \*\* $p < 0.01$ , paired Student  $t$  test.

were significantly higher in TPT-injected mice than in PBS-injected mice (Fig. 3C, 3D). In contrast, the ratio of infiltrated macrophages (F4/80<sup>+</sup> Ly-6G<sup>-</sup>) was comparable between PBS- and TPT-injected mice (Fig. 3C, 3D). Increased infiltration of NK cells (NK1.1<sup>+</sup> CD3<sup>-</sup>) and NKT cells (NK1.1<sup>+</sup> CD3<sup>+</sup>) was not found in TPT-treated mice (Fig. 3C, 3D). Furthermore, immunostaining with anti-CD3 $\zeta$  Ab demonstrated infiltration of CD3 $\zeta$ <sup>+</sup> cells into tumors (Fig. 3E). We next examined whether infiltrated T cells and DCs are activated. Expression of *Irfng* in CD3<sup>+</sup> CD8<sup>+</sup> cells and of *Cd86* in CD11c<sup>+</sup> cells was higher in TPT-treated mice than in PBS-injected mice (Fig. 3F, 3G). Collectively, these findings suggest that TPT has the capacity to drive anti-tumor immunity by recruiting and activating CD8<sup>+</sup> T cells and CD11c<sup>+</sup> DCs.

#### STING is involved in cytokine induction

To understand the molecular mechanisms underlying DC activation by CM from TPT-treated E0771 cells, we used mice deficient for individual PRRs or their signaling molecules. Initially, we evaluated the contributions of TLRs using TLR2 and TLR4 double-KO (DKO) and MyD88 and TRIF-DKO mice. MyD88 and TRIF are adapters for TLRs, and MyD88/TRIF-DKO mice are totally unresponsive to all TLR agonists. IL-6 production was comparable among GM-DCs derived from WT, TLR2/TLR4-DKO, and MyD88/TRIF-DKO mice (Fig. 4A), suggesting that TLRs do not

participate in this response. Next, we investigated the contribution of cytosolic nucleic acid sensors, such as RLRs and DNA sensors. IPS-1 (also known as MAVS) is a sole adapter for RLRs that mediates antiviral innate immune responses, and IPS-1-deficient GM-DCs produced a level of IL-6 comparable to WT mice (Fig. 4B). In contrast, IL-6 production was markedly reduced in GM-DCs from *Sting*<sup>gt/gt</sup> mice (Fig. 4B). mRNA expression of *Il6*, *Cxcl10*, and *Irfn1* was not impaired in IPS-1-deficient GM-DCs, but it was impaired in *Sting*<sup>gt/gt</sup> GM-DCs (Fig. 4C). Furthermore, reduced expression of *Cxcl10* and *Irfn1* mRNAs was also observed in IRF3-deficient GM-DCs (Supplemental Fig. 1B, 1C), suggesting that the STING-IRF3 axis is involved. Therefore, we next examined whether activation of intracellular signaling molecules is impaired in *Sting*<sup>gt/gt</sup> GM-DCs. Phosphorylation of NF- $\kappa$ B and IRF3 after stimulation with CM from TPT-treated E0771 cells was abrogated in *Sting*<sup>gt/gt</sup> GM-DCs (Fig. 4D). In contrast, phosphorylation of ERK1/2, p38, and JNKs was not impaired in *Sting*<sup>gt/gt</sup> GM-DCs (Fig. 4E), suggesting the existence of a STING-independent mechanism of MAPK activation.

It was demonstrated that STING traffics from the endoplasmic reticulum to the Golgi upon stimulation with its agonists (11). We visualized STING by transducing STING-EGFP into MEFs using a retrovirus and found that STING colocalizes with the Golgi after treatment with CM from TPT-treated E0771 cells in a manner similar to ISD stimulation (Fig. 4F). In contrast, STING localized

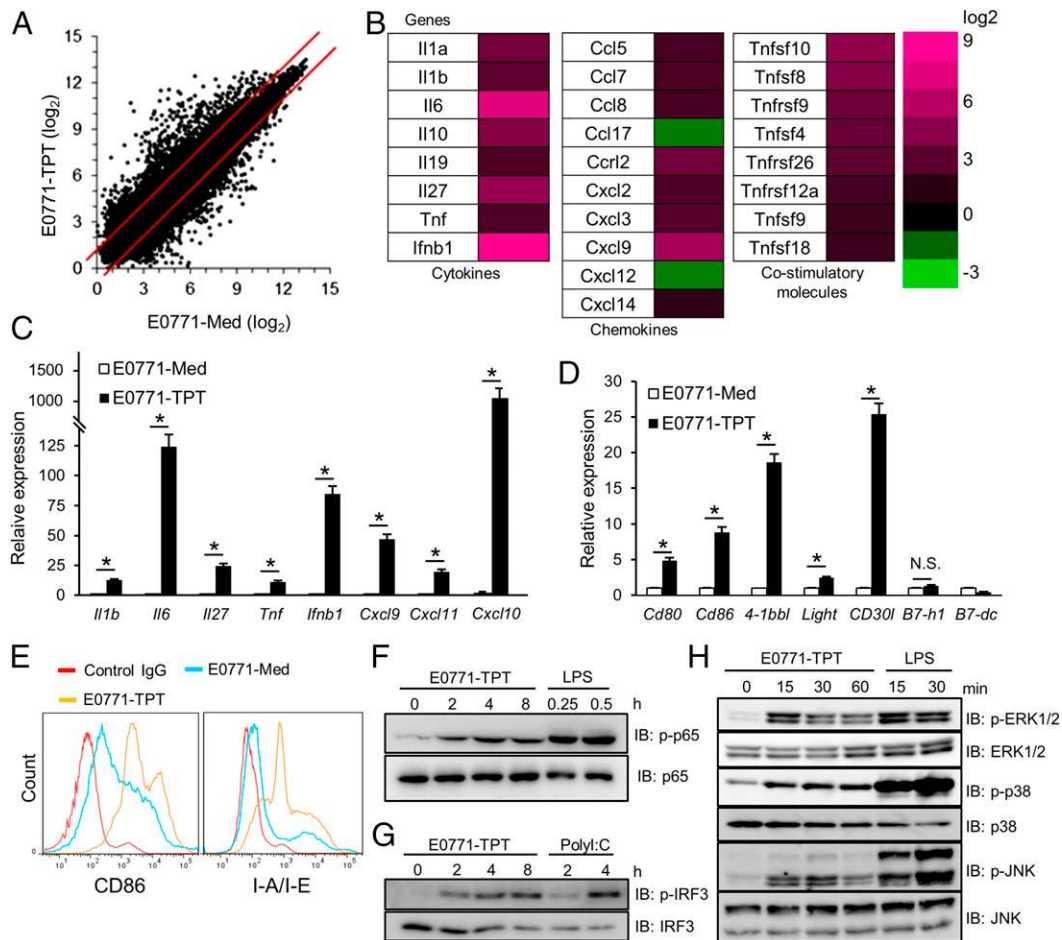


**FIGURE 2.** TPT-induced cell death activates DC maturation and the expression of T cell costimulatory genes. **(A)** GM-DCs were stimulated with CM from E0771 cells for 48 h, and their gene expression was analyzed by microarray. Red lines indicate the thresholds for genes that are upregulated or downregulated  $>2$ -fold after stimulation with CM from TPT-treated E0771 cells. **(B)** Expression of selected genes from **(A)** is shown as heat maps. **(C and D)** Total RNA was extracted as in **(A)**, and gene expression was quantified by qPCR. **(E)** GM-DCs were stimulated as in **(A)**, and the expression of CD86 and I-A/I-E was detected by FACS. **(F–H)** GM-DCs were stimulated with CM from E0771 cells, 100 ng/ml LPS, or 1  $\mu$ g/ml polyI:C for the indicated times, and the cell lysates were blotted with the indicated Abs.  $n = 3$ ; mean values and SEs are depicted.  $*p < 0.05$ , paired Student  $t$  test. N.S., not significant.

as cytoplasmic dot structures, distinct from the Golgi, in MEFs stimulated with CM from untreated E0771 cells (Fig. 4F).

#### Role of STING in TPT-induced antitumor immunity

To understand the contribution of STING to mounting TPT-triggering antitumor immunity against E0771 cells in vivo, we injected E0771 cells into WT and *Sting*<sup>gt/gt</sup> mice and measured tumor volume after treatment with TPT. Tumor growth was severely inhibited by TPT treatment in WT mice, but this inhibition was weaker in *Sting*<sup>gt/gt</sup> mice (Fig. 5A). In contrast, tumor growth after PBS treatment was comparable between WT and *Sting*<sup>gt/gt</sup> mice (Fig. 5A). The number of tumor-infiltrating CD8<sup>+</sup> CD69<sup>+</sup> T cells was higher in WT mice than in *Sting*<sup>gt/gt</sup> mice treated with TPT (Fig. 5B). In addition, expression of *Ifng* by CD3<sup>+</sup> CD8<sup>+</sup> cells and of *Cd86* by CD11c<sup>+</sup> cells was also reduced in TPT-treated *Sting*<sup>gt/gt</sup> mice compared with WT mice (Fig. 5C). These findings suggest that STING is required for the TPT-induced mounting of antitumor immunity in vivo.

#### DNA encapsulated in exosomes released by TPT-treated E0771 cells is immunostimulatory

STING is directly bound and activated by cGAMP, which is produced by cGAS upon DNA ligation. We investigated whether

E0771 cell-derived cGAMP or DNA is responsible for STING activation in DCs. We evaluated the expression of *Mb21d1*, which encodes cGAS, and found that it was much lower in E0771 cells than in GM-DCs and MEFs (Fig. 6A), suggesting that cGAMP is unlikely to be produced by TPT-treated E0771 cells. We then addressed whether cGAS is involved in STING activation in DCs. We suppressed cGAS expression in MEFs by retrovirus-mediated knockdown (Fig. 6B) and found that protein expression of CXCL10 and IL-6 and mRNA expression of *Il6* and *Ifnb* after CM treatment were reduced in cGAS-knockdown cells compared with control cells; their expression after polyI:C treatment was comparable in control and knockdown cells (Fig. 6C, 6D). These results suggest that CM activates the cGAS–STING signaling axis. We then collected DNA from CM from untreated and TPT-treated E0771 cells and used it to transfect GM-DCs by lipofection. IL-6 and CXCL10 production was increased in GM-DCs stimulated with DNA derived from TPT-treated E0771 cells in a dose-dependent manner (Fig. 6E, 6F).

Extracellular DNA is digested by DNases, and mice lacking DNases constitutively induce type I IFNs, which is linked to inflammation and autoimmunity (27, 28). However, we found that DNase treatment of CM from TPT-treated E0771 cells did not influence IL-6 production by DCs (Supplemental Fig. 1D). This

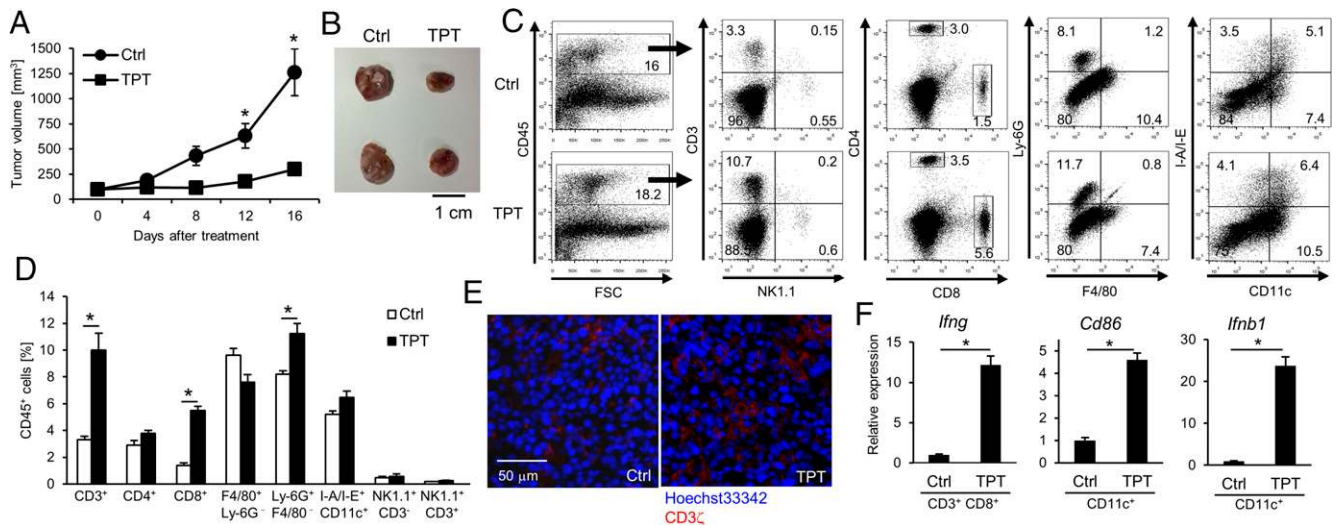


**FIGURE 3.** TPT inhibits E0771 tumor growth. **(A)** E0771 cells were injected s.c. into the right flank of C57BL/6 mice, and PBS or 20 mg/kg TPT was administered i.p. to the mice every 4 d after the tumor volume reached 100 mm<sup>3</sup> (day 0). **(B)** Images of representative E0771 tumors at day 16 from **(A)**. **(C)** and **(D)** E0771 tumors were dissected after intratumoral administration of TPT, and tumor-infiltrating cells were analyzed by FACS. **(E)** Immunostaining of E0771 tumor sections with Hoechst 33342 (blue) and anti-CD3 $\zeta$  (red). **(F)** CD11c<sup>+</sup> or CD3<sup>+</sup> CD8<sup>+</sup> cells were sorted from E0771 tumors, and *Ifng*, *Cd86*, and *Ifnb1* expression was quantified by qPCR.  $n = 4$ ; mean values and SEs are depicted. \* $p < 0.05$ , paired Student  $t$  test.

suggested the possibility that DNA derived from TPT-treated E0771 cells is tightly associated with chromatin proteins, such as HMGB1, that protect DNA from DNase-mediated degradation; however, an anti-HMGB1 Ab that inhibits binding between HMGB1 and its receptor RAGE did not abrogate IL-6 production (Supplemental Fig. 1E). Exosomes are vesicles that are released by many cell types, including cancer cells, and contain various molecules, such as mRNA, microRNA, or membrane proteins (29–31). Recent reports suggested that tumor cells secrete DNA-containing exosomes, but their biological significance remains to be elucidated (3, 32). Therefore, we examined whether DNA-containing exosomes are released upon TPT treatment. We first asked whether exosomes themselves are released following TPT treatment. The exosome fraction was purified from TPT-treated E0771 cells. As shown in Fig. 7A, TPT stimulation increased the quantity of exosomes in the culture supernatant in a time-dependent manner. The purity of exosomes was confirmed by immunoblot analysis with Abs against the exosome marker proteins CD63 and Alix (Fig. 7B). We next determined whether DNA is contained in the exosomes derived from TPT-treated E0771 cells. We purified the exosome fraction and found that DNA was present in exosomes from TPT-treated E0771 cells but not from untreated E0771 cells (Fig. 7C). We then treated E0771 cell-derived exosomes with DNase and observed that DNA fragments having sizes of approximately  $>2$  kbp disappeared after DNase treatment, suggesting that DNA fragments  $< 2$  kbp are trapped in the exosomes. Next, we treated purified exosomes to GM-DCs and examined their ability to induce cytokines. Expression of *Ifnb1*, *Cxcl10*, and *Il6* was upregulated in GM-DCs treated with purified exosomes derived from TPT-treated E0771 cells, and this upregulation was abrogated in *Sting*<sup>gt/gt</sup> GM-DCs (Fig. 7D). In contrast, WT and *Sting*<sup>gt/gt</sup> GM-DCs induced expression of these genes in response to polyI:C, an agonist of RLRs. Likewise, production of IL-6 and CXCL10 was induced by stimulation with the purified exosomes in WT, but not *Sting*<sup>gt/gt</sup>, GM-DCs (Fig. 7E). To explore how DNA in the exosome is delivered to DCs, we analyzed engulfment of the exosome by GM-DCs. We incubated GM-DCs with CSFE-labeled exosomes purified from TPT-treated E0771 cell CM and analyzed their engulfment by FACS analysis. The

labeled exosomes were engulfed when incubated at 37°C, but not at 4°C (Fig. 7F), suggesting that DNA-containing exosomes are incorporated into GM-DCs through an active transport mechanism, such as endocytosis, phagocytosis, or pinocytosis. Furthermore, microscopic analysis demonstrated that labeled exosomes appeared in the cytoplasm as dot-like structures (Fig. 7G). These results suggest that TPT induces the secretion of immunostimulatory DNA-containing exosomes from E0771 cells; these are delivered to the cytoplasm of GM-DCs to activate a STING-dependent pathway.

## Discussion

It has become apparent that DAMPs contribute to antitumor immunity; for example, HSP90 and HMGB1 derived from doxorubicin-treated cancer cells act as TLR agonists in innate immune cells and potentiate antitumor immunity (8, 9). Our study showed that TLRs were dispensable for IL-6 production triggered by TPT. This suggests that HMGB1 and HSP90 from E0771 cells are not released by TPT stimulation, or they are released but are unable to stimulate TLRs as a result of specific modifications or processing that occur through TPT stimulation. In addition, tumor cell-derived ATP was shown to drive NLRP3 inflammasome activation and IL-1 $\beta$  release (5); however, CM from TPT-treated E0771 cells failed to induce IL-1 $\beta$  or IL-33 production by GM-DCs (Fig. 1F), suggesting that the inflammasome is unlikely to participate in TPT-triggered antitumor immune responses. In the current study, we demonstrated that CM from TPT-treated E0771 cells contains immunostimulatory DNA, which activates a STING pathway in DCs and triggers antitumor immune responses. Numerous studies indicated that self-DNA can convert to immunogenic DNA in pathogenic conditions (27, 28). For instance, cells deficient for DNase show aberrant DNA accumulation that is responsible for STING or TLR9 activation and is linked to autoimmunity (27, 28). Moreover, oxidized DNA that is synthesized in cells during radiation exposure is protected from DNase II/Trex I-mediated degradation and contributes to radiation-induced antitumor therapy by activating a STING pathway (10, 13). Therefore, it is thought that TPT stimulation also induces production of DNase-resistant DNA. We found that  $>2$ -kbp DNA from TPT-treated

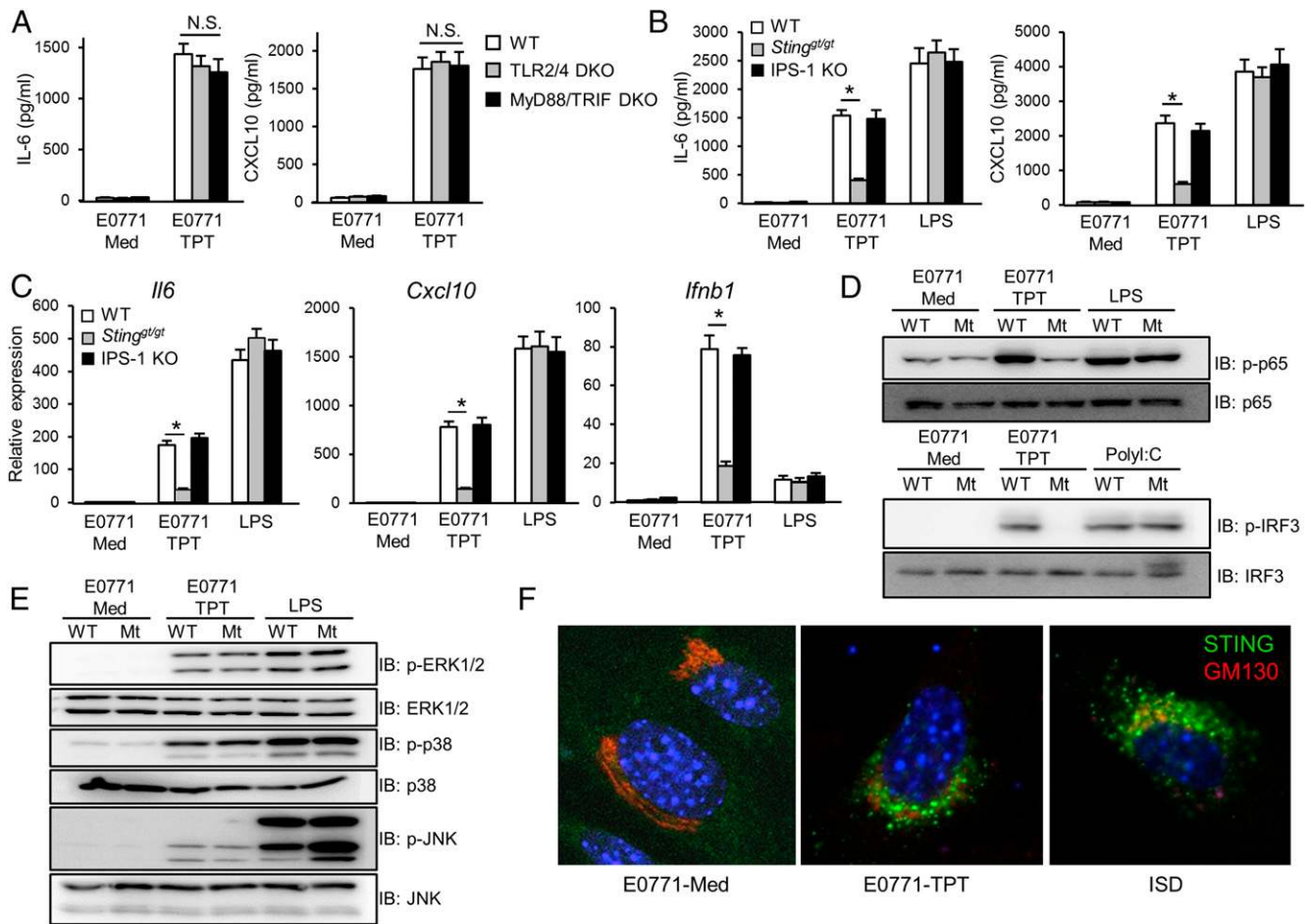


**FIGURE 4.** TPT activates STING signaling through tumor cell death. GM-DCs from the indicated gene-deficient mice were stimulated with CM from E0771 cells for 48 h. Cytokine expression of the GM-DCs was measured by ELISA (**A** and **B**) or qPCR (**C**). (**D** and **E**) WT and *Sting*<sup>g/gt</sup> GM-DCs were stimulated with 100 ng/ml LPS (30 min), 1  $\mu$ g/ml polyI:C (4 h), or CM from E0771 cells for 30 min (p38 MAPK, ERK1/2, JNK) or 4 h (p65, IRF3), and the cell lysates were blotted with the indicated Abs. (**F**) STING-EGFP-expressing MEFs were stimulated with 1  $\mu$ g/ml ISD for 2 h or with CM from E0771 cells for 4 h and then stained with Hoechst 33342 (blue) and anti-GM130 (red). Original magnification  $\times 200$ .  $n = 3$ ; mean values and SEs are depicted. \* $p < 0.05$ , paired Student *t* test. N.S., not significant.

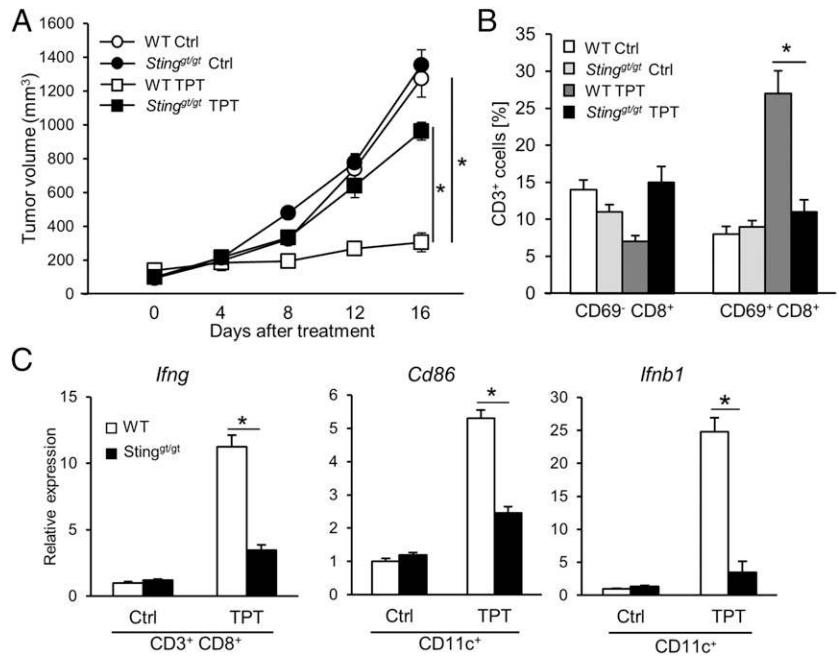
E0771 cells was digested by DNase I treatment (Fig. 7C). However, DNase I treatment failed to inhibit CM-induced IL-6 production in GM-DCs (Supplemental Fig. 1D), suggesting that short DNA fragments in the exosome that were protected from DNase by the exosomal membrane are capable of activating STING. Previous studies showed that exosomes are engulfed by cells through endocytosis or phagocytosis (31, 33). Therefore, it is suggested that the DNA inside exosomes is incorporated into DCs by endocytosis or phagocytosis and traffics to the cytoplasm, activating cGAS–STING signaling.

Topoisomerase I is an enzyme that relaxes supercoiled DNA by introducing single-strand breaks into the DNA helix. During DNA replication, topoisomerase I covalently binds to phosphodiester bonds in DNA, resulting in the formation of topoisomerase I–DNA complexes and induction of single-strand breaks. Because this transient nick is required for the relaxation of supercoiled DNA and the formation of an optimal DNA replication fork, topoisomerase I activity is essential for DNA replication and cellular proliferation (15). The topoisomerase I–induced nick is religated, but this is inhibited by TPT through its intercalation at sites of DNA cleavage. After a DNA-replication fork reaches a TPT-intercalated site, the site is recognized as a DNA double-strand break, which activates DNA damage responses via the ATM/ATR pathway, resulting in p53-mediated apoptosis (34, 35). Our data

suggest that TPT converts cellular DNA into immunostimulatory DNA through TPT-induced cell death and, thus, that the TPT–topoisomerase I–DNA complex is responsible for STING activation, presumably through interaction with the DNA sensor cGAS. Therefore, structure-based analyses of the TPT–topoisomerase I–DNA complex are required to understand how the complex has immunomodulatory activity.

Immunogenic cell death, including necrosis, necroptosis, and pyroptosis, promotes DAMP secretion and innate immune activation (36, 37). TPT induces the death of E0771 cells, but this cell death was not blocked by treatment with caspase-3 inhibitors or RIPK inhibitors or by cotreatment with caspase-3/RIPK inhibitors (Fig. 1G, Supplemental Fig. 2A). These results suggest that TPT-induced cell death is different from apoptosis and necroptosis. Furthermore, CM from TPT-treated E0771 cells was unable to induce IL-1 $\beta$  and IL-18 production and caspase-1 activation (Fig. 1F, Supplemental Fig. 2B, 2C). Therefore, TPT-induced cell death is probably also distinct from pyroptosis. As noted above, previous studies showed that TPT activates DNA damage responses through the ATM/ATR pathway. Although the ATM/ATR pathway promotes p53-mediated apoptosis, our data showed that TPT-induced cell death was probably distinct from conventional caspase-3-dependent apoptosis. Etoposide, a topoisomerase II inhibitor, reportedly induces DNA damage responses via the ATM/ATR

**FIGURE 5.** Tumor growth inhibition by TPT is dependent on STING. **(A)** E0771 cells were injected s.c. into the right flank of C57BL/6 mice, and 20 mg/kg TPT was administered i.p. to the mice every 4 d after the tumor volume reached 100 mm<sup>3</sup> (day 0). **(B)** E0771 tumors were dissected after intratumoral administration of TPT, and tumor-infiltrating cells were analyzed by FACS. **(C)** CD11c<sup>+</sup> or CD3<sup>+</sup> CD8<sup>+</sup> cells were sorted from E0771 tumors, and their expression of *Ifng*, *Cd86*, and *Ifnb1* was quantified by qPCR. *n* = 4; mean values and SEs are depicted. \**p* < 0.05, paired Student *t* test.



pathway and cell death, but CM from etoposide-treated E0771 cells was incapable of activating STING signaling (Fig. 1B) (38). These results suggest that TPT-induced activation of previously unidentified immunogenic cell death pathways, other than ATM/ATR, plays an important role in the production of immunostimulatory DNA.

Numerous studies demonstrated that inflammatory cytokines, including IL-1 $\beta$ , IL-6, and IL-33, contribute to anti- and protumor effects on the tumor environment (39). For instance, IL-6 promotes DC maturation and recruitment of immune cells to tumor sites, which facilitates antitumor immunity. However, it simultaneously increases blood vessel formation in tumors, which supports tumor growth and metastasis (40–42). In contrast, type I IFNs display antitumor properties through facilitating cross-

presentation of tumor Ag by DCs and producing chemokines, such as CXCL9 and CXCL10, which recruit CD8<sup>+</sup> T cells and promote killing of tumor cells (43–45). Moreover, type I IFNs directly inhibit tumor cell proliferation via Rb-mediated cell cycle arrest (46). Our data showed that TPT-treated cells induce the production of inflammatory cytokines, chemokines, and type I IFNs by DCs in a manner dependent on STING, and TPT treatment facilitates CD8<sup>+</sup> T cell infiltration and activation in tumor sites. Indeed, we found that CM stimulation induced type I IFN production and STAT1 phosphorylation (Supplemental Fig. 1A). Upregulation of cGAS, STING, and IRF7 was also observed (Supplemental Fig. 3A). Moreover, IFN- $\beta$  treatment of DCs increased the expression of 4-1bb1, Cd301, Cd86, Il6, Il27, Cxcl9, Cxcl10, and Cxcl11, suggesting that type I IFN induced through

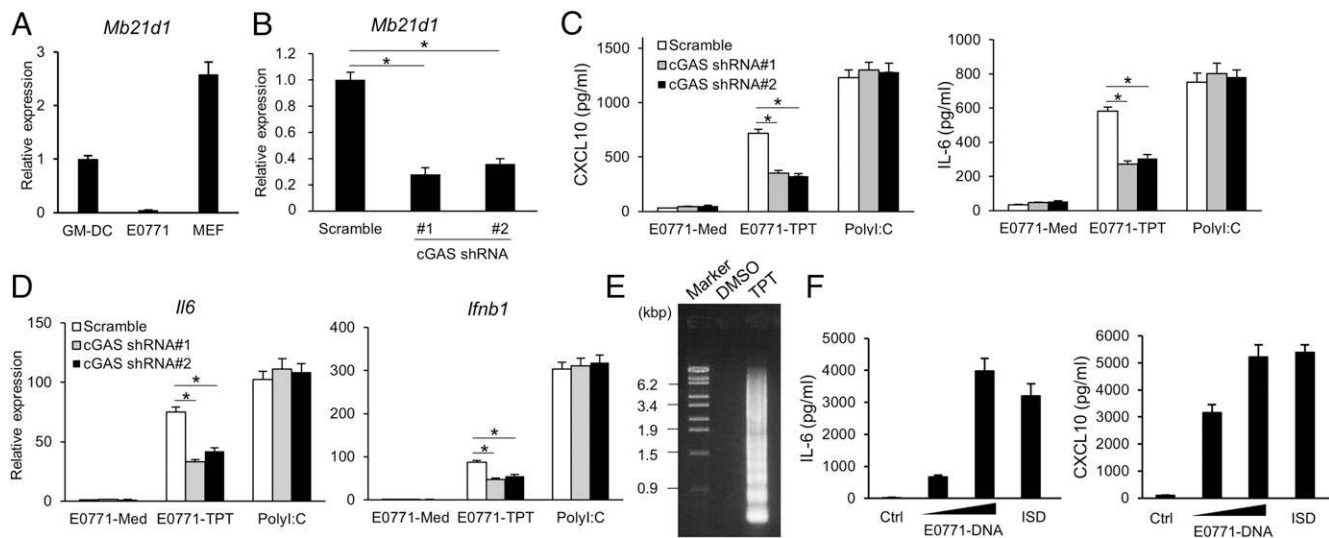


**FIGURE 6.** Immunostimulatory DNA is released from TPT-treated cells. **(A)** Quantification of Mb21d1 mRNA levels by qPCR. **(B)** cGAS was knocked down by shRNA-expressing retrovirus in MEFs, and its knockdown efficiency was quantified by qPCR. **(C)** cGAS-knockdown MEFs were stimulated with CM or 1  $\mu$ g/ml polyI:C for 48 h and then its cytokine production was determined by ELISA. **(D)** cGAS-knockdown MEFs were stimulated with CM for 48 h or with 1  $\mu$ g/ml polyI:C, and its gene expression was measured by qPCR. **(E)** DNA was purified from the CM from TPT-treated E0771 cells and observed by agarose gel electrophoresis. **(F)** GM-DCs were stimulated for 48 h with 0.3 or 1  $\mu$ g/ml DNA from TPT-treated E0771 cells or 1  $\mu$ g/ml ISD, and IL-6 and CXCL10 production was determined by ELISA. *n* = 3; mean values and SEs are depicted. \**p* < 0.05, paired Student *t* test.

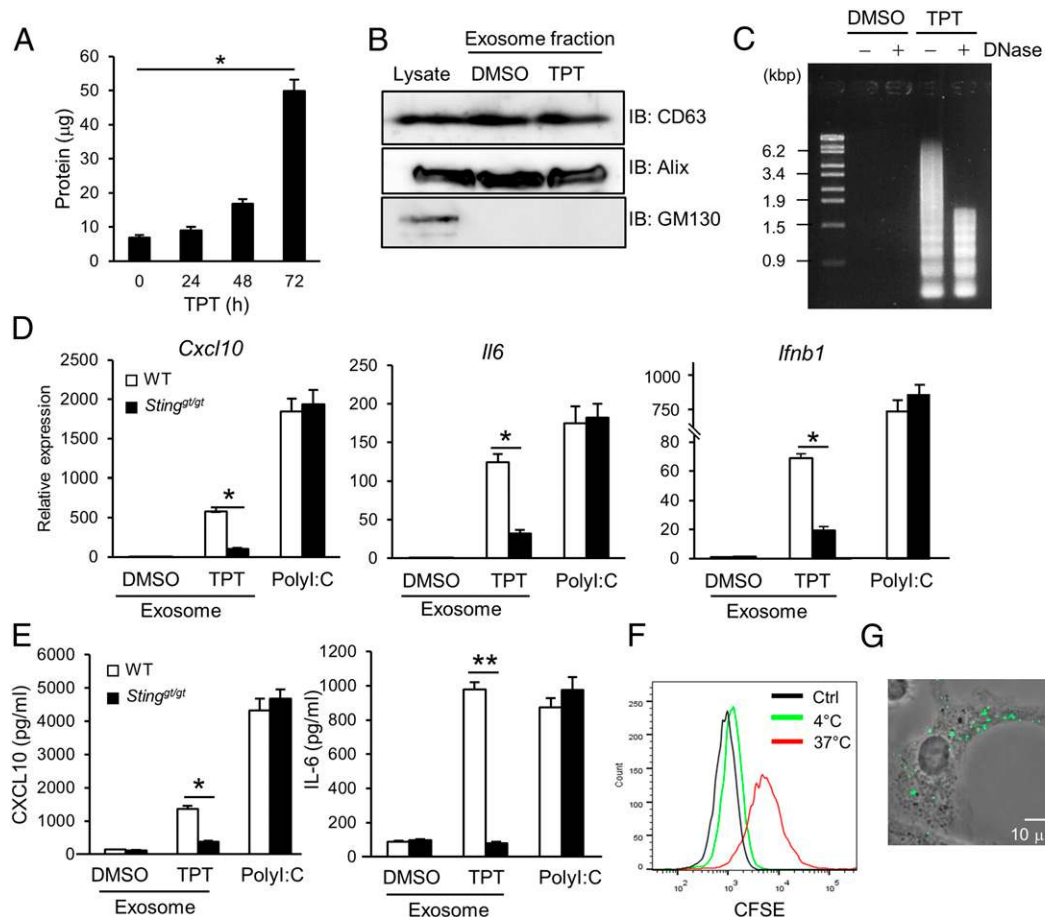


**FIGURE 7.** TPT-treated E0771 cells secrete DNA-containing exosomes. **(A)** E0771 cells were treated with 5 μg/ml TPT for the indicated times, after which the exosome fraction was collected by ultracentrifugation. Purified exosomes were quantified by the Bradford protein assay. **(B)** Exosomes from TPT-treated E0771 cells were immunoblotted with the indicated Abs. **(C)** Exosomes (30 μg per lane) from TPT-treated E0771 cells were treated with 5 U/ml DNase I for 1 h. After phenol/chloroform extraction, the DNA was observed by agarose gel electrophoresis. **(D)** GM-DCs were stimulated with 1 μg/ml polyI:C or 5 μg/ml E0771 cell-derived exosomes for 8 h, and target gene expression was quantified by qPCR. **(E)** GM-DCs were stimulated as in **(D)** for 48 h, and IL-6 and CXCL10 production was determined by ELISA. **(F)** GM-DCs were cultured with 5 μg/ml CFSE-labeled exosomes from TPT-treated E0771 cells for 2 h at 4 or 37°C, and exosome-incorporating cells were quantified by FACS. **(G)** GM-DCs were cultured as in **(F)** at 37°C and then observed by microscopy.  $n = 3$ ; mean values and SEs are depicted. \* $p < 0.05$ , \*\* $p < 0.01$ , paired Student  $t$  test.

the cGAS–STING axis may play central roles in TPT-induced immune responses (Supplemental Fig. 3B). The contribution of neutrophils and macrophages to antitumor immunity remains controversial; numerous reports suggested that they display anti- and protumor effects. They alter the tumor environment by promoting angiogenesis, metastasis, tumor cell killing, and immunosuppression via the production of TGF-β, ROS, VEGF, and leukotrienes (39, 47). TPT treatment did not enhance macrophage infiltration but slightly enhanced neutrophil infiltration into the tumor site (Fig. 3C). These findings implied that neutrophils contribute to TPT-induced antitumor immunity; however, Sting<sup>gt/gt</sup> mice did not exhibit any obvious changes in neutrophil infiltration (data not shown). Therefore, the antitumor effects of TPT may depend primarily on CD8<sup>+</sup> T cells (Fig. 5).

We found that TPT promotes the release of exosomes that contain immunostimulatory DNA. Tumor cell-derived exosomes are known to promote proliferation and metastasis of tumor cells and contain various molecules, such as mRNA, microRNA, or membrane proteins (29–31). Recently, it was reported that several tumor cell lines secrete DNA-containing exosomes, but the biological significance of these observations remains unknown (3, 48, 49). It was suggested that DNA and RNA encapsulated in the exosome play a role in host defense against viral infection. RNA of hepatitis C virus is released as exosomes by infected cells and incorporated by DCs, where it is

recognized by TLR7 and promotes type I IFN-dependent antiviral immunity (33). Moreover, cGAMP was shown to be encapsulated in the exosome in HIV-infected cells and transferred to DCs, which induce type I IFNs via the cGAS–STING pathway (50). Therefore, exosome-mediated nucleic acid recognition in DCs may be a general mechanism to reinforce innate immune responses. Previous studies reported that derivatives of DNA and RNA, including CpG DNA, cGAMP, polyI:C, and ARNAX, activate antitumor immunity by inducing type I IFN production and inhibit tumor growth in murine tumor models (14, 51–53). We presume that DNA-containing exosomes also act as immunostimulators against tumors, because they contain tumor-derived proteins and immunostimulatory DNA and induce modest type I IFN production. Because exosomes generally circulate in blood and have no toxicity, they are ideal carriers of tumor Ags and immunostimulating molecules that are thereby delivered to DCs to efficiently mount antitumor immunity. Taken together, our findings provide an unidentified immunogenic cell death pathway that acts together with secretion of DNA-containing exosomes, which have the possibility to function as unique immunostimulating vesicles.

A previous report suggested that TPT differentially affects the activation of monocyte-derived human DCs, depending on the condition of the DCs. TPT treatment resulted in increased migration

and costimulatory molecule expression of unstimulated DCs, and it prevented the maturation of DCs induced by proinflammatory cytokines through inhibition of NF- $\kappa$ B activity (54). Although the mechanisms underlying how TPT directly activates unstimulated DCs remain unclear, it is possible that the TPT-induced killing of a proportion of DCs, and the subsequent release of DNA, activates surviving DCs. Moreover, a recent report showed that TPT is able to prevent endotoxin-induced septic shock because it inhibits PAMP-induced inflammatory cytokine expression by perturbing topoisomerase I-mediated nucleosome remodeling (55). We also found that cells treated with a high concentration of TPT ( $>15 \mu\text{g/ml}$ ) only modestly induced IL-6 production by DCs (data not shown). Thus, excess amounts of TPT may inhibit innate immune activation because it either promotes excessive cell death, thus producing insufficient immunostimulatory DNA, or it induces topoisomerase I-mediated nucleosome remodeling. Furthermore, in vivo, high levels of TPT may suppress antitumor immunity by inducing cell death of proliferating immune cells, such as T cells, which is a common occurrence during treatment with chemotherapeutic agents (56). Therefore, the balance between TPT-induced immune activation and suppression should be carefully controlled to optimize antitumor immunity.

## Acknowledgments

We thank K. Abe for secretarial assistance, T. Kusakabe for technical assistance, and M. Takahama and Dr. T. Oshima for helpful discussions.

## Disclosures

The authors have no financial conflicts of interest.

## References

- Kawai, T., and S. Akira. 2011. Toll-like receptors and their crosstalk with other innate receptors in infection and immunity. *Immunity* 34: 637–650.
- Crîșan, T. O., M. G. Netea, and L. A. Joosten. 2016. Innate immune memory: implications for host responses to damage-associated molecular patterns. *Eur. J. Immunol.* 46: 817–828.
- Guescini, M., D. Guidolin, L. Vallorani, L. Casadei, A. M. Gioacchini, P. Tibollo, M. Battistelli, E. Falcieri, L. Battistin, L. F. Agnati, and V. Stocchi. 2010. C2C12 myoblasts release micro-vesicles containing mtDNA and proteins involved in signal transduction. *Exp. Cell Res.* 316: 1977–1984.
- McCarthy, C. M., and L. C. Kenny. 2016. Immunostimulatory role of mitochondrial DAMPs: alarming for pre-eclampsia? *Am. J. Reprod. Immunol.* 76: 341–347.
- Pandolfi, F., S. Altamura, S. Frosali, and P. Conti. 2016. Key role of DAMP in inflammation, cancer, and tissue repair. *Clin. Ther.* 38: 1017–1028.
- Kawai, T., and S. Akira. 2010. The role of pattern-recognition receptors in innate immunity: update on Toll-like receptors. *Nat. Immunol.* 11: 373–384.
- Zou, J., T. Kawai, T. Tsuchida, T. Kozaki, H. Tanaka, K. S. Shin, H. Kumar, and S. Akira. 2013. Poly IC triggers a cathepsin D- and IPS-1-dependent pathway to enhance cytokine production and mediate dendritic cell necroptosis. *Immunity* 38: 717–728.
- Ma, Y., S. Adjemian, S. R. Mattarollo, T. Yamazaki, L. Aymeric, H. Yang, J. P. Portela Catani, D. Hannani, H. Duret, K. Steegh, et al. 2013. Anticancer chemotherapy-induced intratumoral recruitment and differentiation of antigen-presenting cells. *Immunity* 38: 729–741.
- Fucikova, J., P. Kralikova, A. Fialova, T. Brtnicky, L. Rob, J. Bartunkova, and R. Spisek. 2011. Human tumor cells killed by anthracyclines induce a tumor-specific immune response. *Cancer Res.* 71: 4821–4833.
- Gehrke, N., C. Mertens, T. Zillinger, J. Wenzel, T. Bald, S. Zahn, T. Tüting, G. Hartmann, and W. Barchet. 2013. Oxidative damage of DNA confers resistance to cytosolic nuclease TREX1 degradation and potentiates STING-dependent immune sensing. *Immunity* 39: 482–495.
- Cai, X., Y. H. Chiu, and Z. J. Chen. 2014. The cGAS-cGAMP-STING pathway of cytosolic DNA sensing and signaling. *Mol. Cell* 54: 289–296.
- Woo, S. R., M. B. Fuentes, L. Corrales, S. Spranger, M. J. Furdyna, M. Y. Leung, R. Duggan, Y. Wang, G. N. Barber, K. A. Fitzgerald, et al. 2014. STING-dependent cytosolic DNA sensing mediates innate immune recognition of immunogenic tumors. [Published erratum appears in 2015 *Immunity* 42: 199.] *Immunity* 41: 830–842.
- Deng, L., H. Liang, M. Xu, X. Yang, B. Burnette, A. Arina, X. D. Li, H. Mauceri, M. Beckett, T. Darga, et al. 2014. STING-dependent cytosolic DNA sensing promotes radiation-induced type I interferon-dependent antitumor immunity in immunogenic tumors. *Immunity* 41: 843–852.
- Demaria, O., A. De Gassart, S. Coso, N. Gestermann, J. Di Domizio, L. Flatz, O. Gaide, O. Michielin, P. Hwu, T. V. Petrova, et al. 2015. STING activation of tumor endothelial cells initiates spontaneous and therapeutic antitumor immunity. *Proc. Natl. Acad. Sci. USA* 112: 15408–15413.
- Staker, B. L., K. Hjerrild, M. D. Feese, C. A. Behnke, A. B. Burgin, Jr., and L. Stewart. 2002. The mechanism of topoisomerase I poisoning by a camptothecin analog. *Proc. Natl. Acad. Sci. USA* 99: 15387–15392.
- Sauer, J. D., K. Sotelo-Troha, J. von Moltke, K. M. Monroe, C. S. Rae, S. W. Brubaker, M. Hyodo, Y. Hayakawa, J. J. Woodward, D. A. Portnoy, and R. E. Vance. 2011. The N-ethyl-N-nitrosourea-induced goldenticket mouse mutant reveals an essential function of Sting in the in vivo interferon response to *Listeria monocytogenes* and cyclic dinucleotides. *Infect. Immun.* 79: 688–694.
- Kawai, T., O. Adachi, T. Ogawa, K. Takeda, and S. Akira. 1999. Unresponsiveness of MyD88-deficient mice to endotoxin. *Immunity* 11: 115–122.
- Yamamoto, M., S. Sato, H. Hemmi, K. Hoshino, T. Kaisho, H. Sanjo, O. Takeuchi, M. Sugiyama, M. Okabe, K. Takeda, and S. Akira. 2003. Role of adaptor TRIF in the MyD88-independent toll-like receptor signaling pathway. *Science* 301: 640–643.
- Takeuchi, O., K. Hoshino, T. Kawai, H. Sanjo, H. Takada, T. Ogawa, K. Takeda, and S. Akira. 1999. Differential roles of TLR2 and TLR4 in recognition of gram-negative and gram-positive bacterial cell wall components. *Immunity* 11: 443–451.
- Hoshino, K., O. Takeuchi, T. Kawai, H. Sanjo, T. Ogawa, Y. Takeda, K. Takeda, and S. Akira. 1999. Cutting edge: toll-like receptor 4 (TLR4)-deficient mice are hyporesponsive to lipopolysaccharide: evidence for TLR4 as the Lps gene product. *J. Immunol.* 162: 3749–3752.
- Kumar, H., T. Kawai, H. Kato, S. Sato, K. Takahashi, C. Coban, M. Yamamoto, S. Uematsu, K. J. Ishii, O. Takeuchi, and S. Akira. 2006. Essential role of IPS-1 in innate immune responses against RNA viruses. *J. Exp. Med.* 203: 1795–1803.
- Sato, M., H. Suemori, N. Hata, M. Asagiri, K. Ogasawara, K. Nakao, T. Nakaya, M. Katsuki, S. Noguchi, N. Tanaka, and T. Taniguchi. 2000. Distinct and essential roles of transcription factors IRF-3 and IRF-7 in response to viruses for IFN- $\alpha$ / $\beta$  gene induction. *Immunity* 13: 539–548.
- Kitai, Y., O. Takeuchi, T. Kawasaki, D. Ori, T. Sueyoshi, M. Murase, S. Akira, and T. Kawai. 2015. Negative regulation of melanoma differentiation-associated gene 5 (MDA5)-dependent antiviral innate immune responses by Arf-like protein 5B. *J. Biol. Chem.* 290: 1269–1280.
- Saitoh, T., N. Fujita, T. Hayashi, K. Takahara, T. Satoh, H. Lee, K. Matsunaga, S. Kageyama, H. Omori, T. Noda, et al. 2009. Atg9a controls dsDNA-driven dynamic translocation of STING and the innate immune response. *Proc. Natl. Acad. Sci. USA* 106: 20842–20846.
- Tanaka, H., H. Matsushima, A. Nishibu, B. E. Clausen, and A. Takashima. 2009. Dual therapeutic efficacy of vinblastine as a unique chemotherapeutic agent capable of inducing dendritic cell maturation. *Cancer Res.* 69: 6987–6994.
- Zitvogel, L., L. Apetoh, F. Ghiringhelli, and G. Kroemer. 2008. Immunological aspects of cancer chemotherapy. *Nat. Rev. Immunol.* 8: 59–73.
- Stetson, D. B., J. S. Ko, T. Heidmann, and R. Medzhitov. 2008. Trex1 prevents cell-intrinsic initiation of autoimmunity. *Cell* 134: 587–598.
- Kawane, K., H. Fukuyama, G. Kondoh, J. Takeda, Y. Ohsawa, Y. Uchiyama, and S. Nagata. 2001. Requirement of DNase II for definitive erythropoiesis in the mouse fetal liver. *Science* 292: 1546–1549.
- Tominaga, N., N. Kosaka, M. Ono, T. Katsuda, Y. Yoshioka, K. Tamura, J. Lötvall, H. Nakagawa, and T. Ochiya. 2015. Brain metastatic cancer cells release microRNA-181c-containing extracellular vesicles capable of destructing blood-brain barrier. *Nat. Commun.* 6: 6716.
- Kosaka, N. 2016. Decoding the secret of cancer by means of extracellular vesicles. *J. Clin. Med.* 5: 22.
- Hoshino, A., B. Costa-Silva, T. L. Shen, G. Rodrigues, A. Hashimoto, M. Tesic Mark, H. Molina, S. Kohsaka, A. Di Giannatale, S. Ceder, et al. 2015. Tumour exosome integrins determine organotropic metastasis. *Nature* 527: 329–335.
- Thakur, B. K., H. Zhang, A. Becker, I. Matei, Y. Huang, B. Costa-Silva, Y. Zheng, A. Hoshino, H. Brazier, J. Xiang, et al. 2014. Double-stranded DNA in exosomes: a novel biomarker in cancer detection. *Cell Res.* 24: 766–769.
- Dreux, M., U. Garaigorta, B. Boyd, E. Décembre, J. Chung, C. Whitten-Bauer, S. Wieland, and F. V. Chisari. 2012. Short-range exosomal transfer of viral RNA from infected cells to plasmacytoid dendritic cells triggers innate immunity. *Cell Host Microbe* 12: 558–570.
- Cliby, W. A., K. A. Lewis, K. K. Lilly, and S. H. Kaufmann. 2002. S phase and G2 arrests induced by topoisomerase I poisons are dependent on ATR kinase function. *J. Biol. Chem.* 277: 1599–1606.
- Tanaka, T., A. Kurose, X. Huang, W. Dai, and Z. Darzynkiewicz. 2006. ATM activation and histone H2AX phosphorylation as indicators of DNA damage by DNA topoisomerase I inhibitor topotecan and during apoptosis. *Cell Prolif.* 39: 49–60.
- Jorgensen, I., and E. A. Miao. 2015. Pyroptotic cell death defends against intracellular pathogens. *Immunity* 43: 130–142.
- Yatim, N., H. Jusforgues-Saklani, S. Orozco, O. Schulz, R. Barreira da Silva, C. Reis e Sousa, D. R. Green, A. Oberst, and M. L. Albert. 2015. RIPK1 and NF- $\kappa$ B signaling in dying cells determines cross-priming of CD8<sup>+</sup> T cells. *Science* 350: 328–334.
- Wei, F., Y. Xie, L. Tao, and D. Tang. 2010. Both ERK1 and ERK2 kinases promote G2/M arrest in etoposide-treated MCF7 cells by facilitating ATM activation. *Cell. Signal.* 22: 1783–1789.
- Shalapour, S., and M. Karin. 2015. Immunity, inflammation, and cancer: an eternal fight between good and evil. *J. Clin. Invest.* 125: 3347–3355.
- Song, L., M. A. Smith, P. Doshi, K. Sasser, W. Fulp, S. Altiock, and E. B. Haura. 2014. Antitumor efficacy of the anti-interleukin-6 (IL-6) antibody siltuximab in mouse xenograft models of lung cancer. *J. Thorac. Oncol.* 9: 974–982.

41. Hodge, D. R., E. M. Hurt, and W. L. Farrar. 2005. The role of IL-6 and STAT3 in inflammation and cancer. *Eur. J. Cancer* 41: 2502–2512.
42. Wei, L. H., M. L. Kuo, C. A. Chen, C. H. Chou, K. B. Lai, C. N. Lee, and C. Y. Hsieh. 2003. Interleukin-6 promotes cervical tumor growth by VEGF-dependent angiogenesis via a STAT3 pathway. *Oncogene* 22: 1517–1527.
43. Fuertes, M. B., S. R. Woo, B. Burnett, Y. X. Fu, and T. F. Gajewski. 2013. Type I interferon response and innate immune sensing of cancer. *Trends Immunol.* 34: 67–73.
44. Rizza, P., F. Moretti, I. Capone, and F. Belardelli. 2015. Role of type I interferon in inducing a protective immune response: perspectives for clinical applications. *Cytokine Growth Factor Rev.* 26: 195–201.
45. Liu, M., S. Guo, and J. K. Stiles. 2011. The emerging role of CXCL10 in cancer (Review). *Oncol. Lett.* 2: 583–589.
46. Sangfelt, O., S. Erickson, and D. Grandér. 2000. Mechanisms of interferon-induced cell cycle arrest. *Front. Biosci.* 5: D479–D487.
47. Bonavita, O., M. Massara, and R. Bonecchi. 2016. Chemokine regulation of neutrophil function in tumors. *Cytokine Growth Factor Rev.* 30: 81–86.
48. Lespagnol, A., D. Duflaut, C. Beekman, L. Blanc, G. Fiucci, J. C. Marine, M. Vidal, R. Amson, and A. Telerman. 2008. Exosome secretion, including the DNA damage-induced p53-dependent secretory pathway, is severely compromised in TSAP6/Steap3-null mice. *Cell Death Differ.* 15: 1723–1733.
49. Guescini, M., S. Genedani, V. Stocchi, and L. F. Agnati. 2010. Astrocytes and glioblastoma cells release exosomes carrying mtDNA. *J. Neural Transm. (Vienna)* 117: 1–4.
50. Bridgeman, A., J. Maelfait, T. Davenne, T. Partridge, Y. Peng, A. Mayer, T. Dong, V. Kaeffer, P. Borrow, and J. Rehwinkel. 2015. Viruses transfer the antiviral second messenger cGAMP between cells. *Science* 349: 1228–1232.
51. Whitmore, M. M., M. J. DeVeer, A. Edling, R. K. Oates, B. Simons, D. Lindner, and B. R. Williams. 2004. Synergistic activation of innate immunity by double-stranded RNA and CpG DNA promotes enhanced antitumor activity. *Cancer Res.* 64: 5850–5860.
52. Cheng, Y. S., and F. Xu. 2010. Anticancer function of polyinosinic-polycytidylic acid. *Cancer Biol. Ther.* 10: 1219–1223.
53. Matsumoto, M., M. Tatematsu, F. Nishikawa, M. Azuma, N. Ishii, A. Morii-Sakai, H. Shime, and T. Seya. 2015. Defined TLR3-specific adjuvant that induces NK and CTL activation without significant cytokine production in vivo. *Nat. Commun.* 6: 6280.
54. Trojandt, S., D. Knies, S. Pektor, S. Ritz, V. Mailänder, S. Grabbe, A. B. Reske-Kunz, and M. Bros. 2013. The chemotherapeutic agent topotecan differentially modulates the phenotype and function of dendritic cells. *Cancer Immunol. Immunother.* 62: 1315–1326.
55. Rialdi, A., L. Campisi, N. Zhao, A. C. Lagda, C. Pietzsch, J. S. Ho, L. Martinez-Gil, R. Fenouil, X. Chen, M. Edwards, et al. 2016. Topoisomerase 1 inhibition suppresses inflammatory genes and protects from death by inflammation. *Science* 352: aad7993.
56. Barreto, J. N., K. B. McCullough, L. L. Ice, and J. A. Smith. 2014. Antineoplastic agents and the associated myelosuppressive effects: a review. *J. Pharm. Pract.* 27: 440–446.